Bojan ŠTUMBERGER[1,2], Miralem HADŽISELIMOVIĆ[1,2], Gorazd HREN[1]

University of Maribor, Faculty of Energy Technology (1)
University of Maribor, Faculty of Electrical Engineering and Computer Science (2)

Design of fractional-slot permanent magnet synchronous motor with concentrated windings and interior permanent magnets

Abstract. The paper presents design of fractional-slot permanent magnet synchronous motors with concentrated windings and interior permanent magnets. Inner PM rotor machines with 12 slot/8 poles and 12 slot/10 poles were investigated. Finite element analysis is employed in order to determine the performance of each motor. It is shown that the maximal torque capability and the flux-weakening performance of the particular machine are strongly dependent on the stator slot number/rotor pole number combination, rotor barrier design and on the quality of used PM material.

Streszczenie. W artykule przedstawiono projekt silnika synchronicznego z magnesami trwałymi (IPMSM) o uzwojeniu ułamkowo-żłobkowym. Badaniom poddano maszyny PMSM o stosunku żłobki/bieguny 12/8 oraz 12/10. Zastosowano analizę metodą elementów skończonych. Wykazano, że maksymalny moment mechaniczny oraz osłabianie strumienia są silnie zależne od stosunku ilości żłobków stojana do liczby par biegunów wirnika oraz jakości materiałów. (Projekt silnika synchronicznego z magnesami trwałymi zagłębionymi w wirniku o uzwojeniu ułamkowo-żłobkowym skupionym).

Keywords: synchronous machine, interior permanent magnets, concentrated windings.
Słowa kluczowe: maszyna synchrnoniczna, magnesy trwałe zagłębione w wirniku, uzwojenie skupione.

Introduction

Fractional-slot permanent magnet (PM) synchronous motors with concentrated windings have in recent years received particular attention due to several important advantages in comparison to the machines with distributed windings. These advantages can be shortly assembled in the following sentences: shorter end winding length when the machine is built in concentrated non-overlapping stator windings technology; higher slot fill factor in comparison to the machines with distributed windings; good flux weakening performance; high torque and fault tolerant capability; good efficiency, etc. [1-8].

The main disadvantages of fractional-slot PM machines with concentrated windings are as following: stator magnetomotive force (MMF) distribution contains a large number of space harmonics; lower and higher order stator MMF harmonics, rotating at speeds different from the rotor speed, cause localised core saturation, higher iron core losses and eddy current loss in permanent magnets [8].

While the use of fractional-slot PM machines with surface mounted PMs is quite frequent, the use of fractional-slot PM machines built in concentrated non-overlapping stator technology with rotor magnets buried inside the rotor construction is still limited. Due to the significant inter-pole leakage flux the buried PM machines are normally equipped with strong Nd-Fe-B magnets in order to minimize the influence of inter-pole leakage effect on the machine performance. However, the price of the Nd-Fe-B magnet has increased significantly during the last two years. Therefore, it would be interesting and important to substitute expensive Nd-Fe-B magnets with cheaper ferrite magnets without significant loss of machine performance. The goal of this paper is the attempt to fill the gap in this field.

The commercial three-phase interior PM machine with Nd-Fe-B magnets and following nominal data was selected as the base motor for this study: one phase voltage supply for power electronics 230 V, nominal output torque 1.5 Nm (overload torque 3 Nm) at nominal speed 525 rpm and minimal torque of 0.34 Nm at maximal speed 16000 rpm, stator diameter 92 mm, rotor diameter 45 mm, machine core length 50 mm, natural cooling, 12 slot/8 pole, concentrated winding technology in star winding connection.

Ferrite magnets have a significantly lower maximal energy product than Nd-Fe-B magnets, therefore the interior PM machine design with ferrite magnets will demand increasing of rotor diameter in order to achieve requested torque within normal current density level in stator windings. Increasing of rotor diameter, however, is limited due to the mechanical strength of the rotor bridges above magnet segments in rotor construction, which have to be designed with particular care in order to maintain mechanical strength of the rotor construction and minimize the inter-pole leakage simultaneously. The additional cost of the increased machine volume can be compensated with replacement of copper wire with aluminium wire. During the design of interior PM motor with ferrite magnets the existent power electronics current limit of 4.46 A was fully taken into account.

According to all mentioned limitations, the interior PM motor with ferrite magnets and aluminium wire has been designed and compared with commercial interior PM with Nd-Fe-B magnets and copper wire. Two different slot/pole number combinations for interior PM motor with ferrite magnets and aluminium wire were taken into account: 12 slot/8 pole design and 12 slot/10 pole design.

Machine characteristics were calculated by using 2D finite element method software by taking into account copper loss, iron core losses and friction and windage losses. The measured machine characteristics of built 12 slot/10 pole prototype machine with ferrite magnets and aluminium wire are presented at the end of this paper.

Method of analysis

The calculation of magnetic conditions:

To obtain the field distributions and the loci of local flux density vectors in the motor, a series of magneto-static field calculations for a complete cycle of field variation was computed by 2D FEM, using the basic equation:

$$(1) \qquad \mathrm{rot}(\nu\mathrm{rot}(\boldsymbol{A})) = \boldsymbol{J}_0 + \mathrm{rot}\boldsymbol{M}$$

where ν denotes the reluctivity, $\boldsymbol{A}$ is the magnetic vector potential, $\boldsymbol{J}_0$ is the current density and $\boldsymbol{M}$ is the magnetization of the permanent magnets.

The non-linearity of the used iron core material was accounted for with a single-valued *B-H* curve, although

more sophisticated models for description of iron core material could be used [9-12]. The magnetic conditions over a complete cycle of magnetic field variation were calculated in discrete equidistant time steps by shifting the rotor position and simultaneously changing the stator excitation [13, 14].

Terminal voltage and input power calculation:
The discrete time forms of phase voltages were calculated from the average values of the vector magnetic potential in stator slots according to the winding arrangement scheme. The end winding contribution was taken into consideration with the constant value of end winding inductance L_e.

The instantaneous value of the phase voltage in the winding of phase a is given by

$$(2) \qquad v_a(t) = Ri_a(t) + \frac{p}{c}\frac{d\psi_{ap}(t)}{dt} + L_e\frac{di_a(t)}{dt}$$

where R is phase resistance, ψ_{ap} is the instantaneous flux linkage of the a phase winding per pole, p is the number of pole pairs and c is the number of parallel circuit of the phase winding. Terminal line-to-line voltage was calculated from calculated waveforms of phase voltages.

The input power was calculated from calculated time forms of phase voltages and the known form of input current as

$$(3) \qquad P_1 = \frac{1}{T}\int_o^T \left[v_a(t)i_a(t) + v_b(t)i_b(t) + v_c(t)i_c(t) \right]dt$$

The iron loss calculation:
An arbitrary flux density vector variation in each element of mesh was expanded into a Fourier series of elliptical harmonic flux density vectors. The total core loss in each element of mesh was determined as the sum of total hysteresis losses p_{th}, total classical eddy current losses p_{te} and total excess losses p_{ta} [14-16].

Efficiency determination:
Efficiency in motor and generator mode of operation was determined by the following equations:

$$(4) \qquad \eta_{mot} = \frac{T_{el}\omega_{mec} - P_{fe} - P_{fw}}{T_{el}\omega_{mec} + P_{cu}}$$

where T_{el} is electromagnetic torque, ω_{mec} is shaft angular speed, P_{cu} are joule losses, P_{fe} are iron core losses and P_{fw} are friction and windage losses.

Mechanical strength of the rotor structure
Magnitude of mechanical deformation and nodal value of stress tensor component at maximal speed of 16000 rpm were determined for each rotor structure.

Results and discussion
According to the current limits of power electronics, according to the sufficient mechanical strength of the rotor structure and according to the torque demands, the outer rotor diameter of the interior PM machine with ferrite magents and aluminium wire was limited to the 65 mm, while the outer stator diameter was limited to the 110 mm. The minimal thickness of the rotor bridges between the rotor poles was limited to 1 mm, while the minimal thickness of the rotor bridges above the magnet pole was limited to the 0.4 mm. The axial length of the machine was limited to the 50 mm.

All machines have to exhibit sinusoidal-shape phase back-EMF waveform and minimal torque ripple at low and high speed. These requests were satisfied by the non-uniform air-gap design and appropriate width and thickness of the PM material.

Cross-sections of interior PM motors which satisfied electromagnetic design requirements were presented in Fig. 1. Magnitude of mechanical deformation and nodal value of stress tensor component at speed of 16000 rpm were determined for 12 slot/8 pole and 12 slot/10 pole rotor structures with ferrite magnets and outer rotor diameter of 65 mm. While the 12 slot/10 pole machine satisfied mechanical requirements (reasonable maximal deformation and maximal mechanical stress component below $2.8{*}10^8$ N/m^2), the maximal value of calculated mechanical stress component in 12 slot/8 pole machine with ferrite magnets is $3.26{*}10^8$ N/m^2 and exceeds $2.8{*}10^8$ N/m^2 value of material. Results of mechanical deformation and results of the stress analysis for the 12 slot/10 pole machine are presented in Figs. 2 and 3. In Figs. 4 and 5, the magnetic flux density distribution in 12 slot/8 pole interior PM motor with Nd-Fe-B magnets for nominal load of 1.5 Nm and overload of 3 Nm are presented. The magnetic flux density distributions for 12 slot/10 pole motor with ferrite magnets are presented in Figs. 6-8.
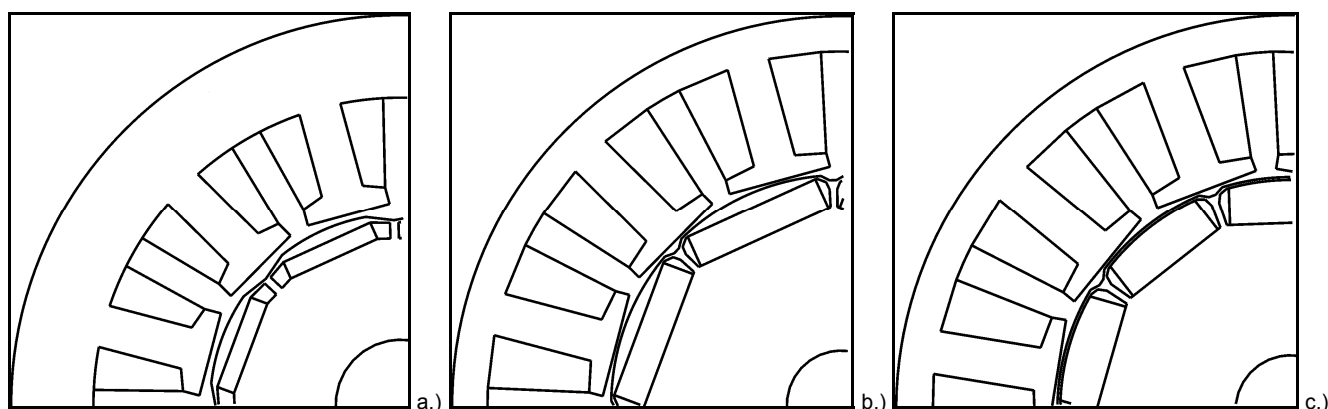
Fig. 1. Machine cross-section: (a) 12 slot/8 pole PM machine with Nd-Fe-B magnets (minimal one side air-gap 0.75 mm); (b) 12 slot/8 pole PM machine with ferrite magnets (minimal one side air-gap 0.4 mm); (c) 12 slot/10 pole PM machine with ferrite magnets (minimal one side air-gap 0.4 mm).
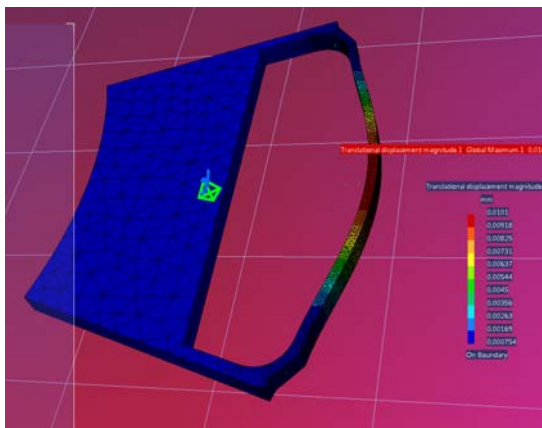
Fig. 2. Maximal calculated mechanical deformation 0.0101194 mm, 12 slot/10 pole machine at 16000 rpm.
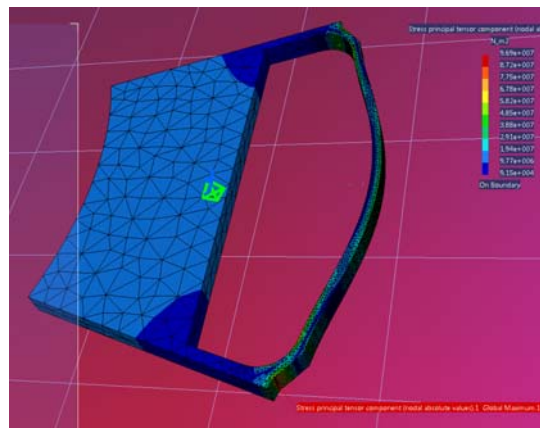
Fig. 3. Maximal nodal value of mechanical stress tensor component $9.67*10^7$ N/m^2, 12 slot/10 pole machine at 16000 rpm.
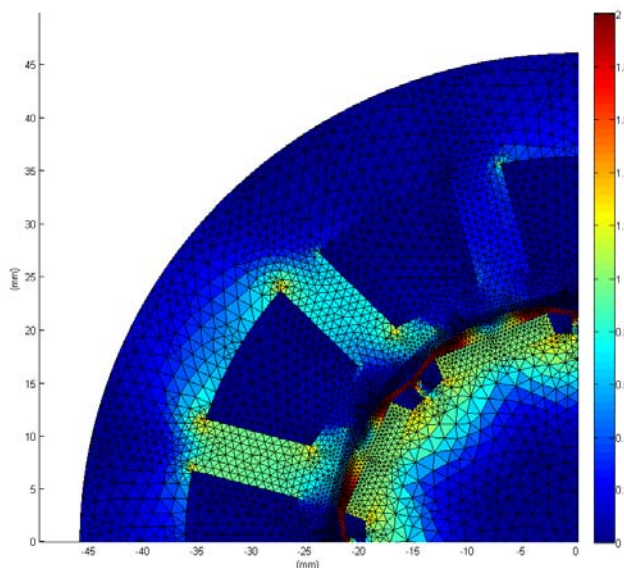
Fig. 4. Magnetic flux density distribution over the machine cross section at 1.5 Nm, 12 slot/8 pole motor, Nd-Fe-B magnets.
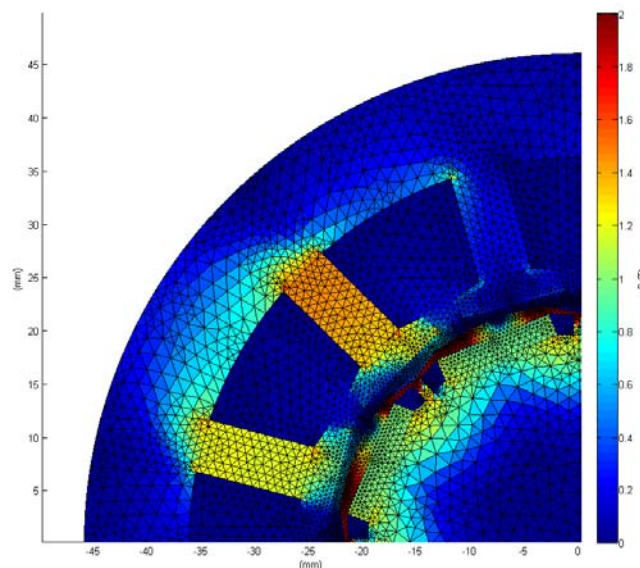
Fig. 5. Magnetic flux density distribution over the machine cross section at 3.0 Nm, 12 slot/8 pole motor, Nd-Fe-B magnets.
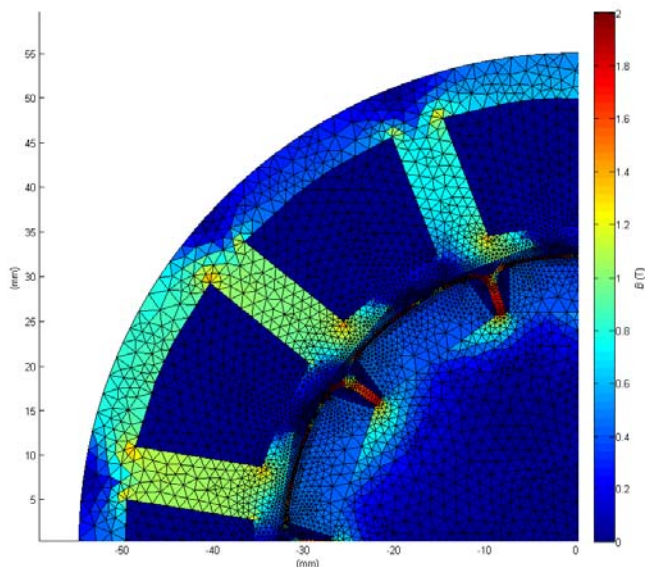
Fig. 6. Magnetic flux density distribution over the machine cross section at 1.5 Nm, 12 slot/10 pole motor, ferrite magnets.
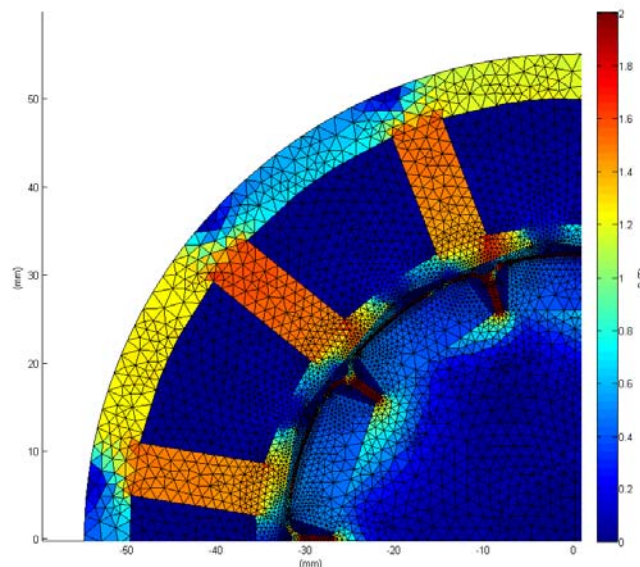
Fig. 7. Magnetic flux density distribution over the machine cross section at 3.0 Nm, 12 slot/10 pole motor, ferrite magnets.
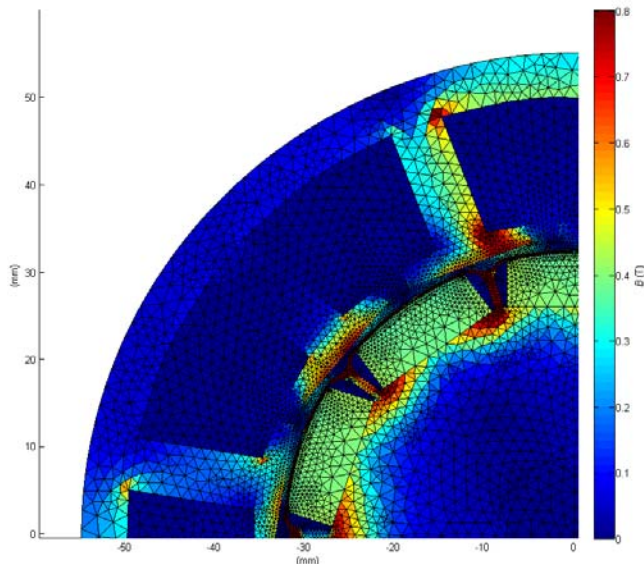
Fig. 8. Magnetic flux density distribution over the machine cross section at 0.367 Nm, flux weakening at 15000 rpm, 12 slot/10 pole motor, ferrite magnets.

According to the calculation results the 12 slot/10 pole machine was manufactured and tested (outer stator diameter 110 mm, rotor outer diameter 65 mm, axial length 50 mm). Measured results of 12 slot/10 pole machine with ferrite magnets are presented in Figs. 9 and 10. Due to the limitation of measured equipment the measurements were performed in limited speed range between 3000 and 15000 rpm at constant RMS value of line-to-line voltage 200 V.
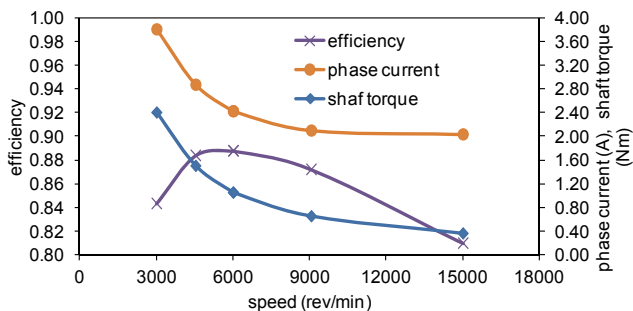
Fig. 9. Efficiency, phase current and shaft torque in dependency on speed for 12 slot/10 pole motor, ferrite magnets, maximal torque at constant RMS value of line-to-line voltage 200 V.
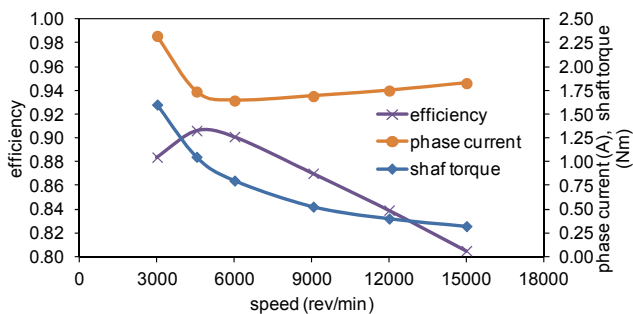
Fig. 10. Efficiency, phase current and shaft torque in dependency on speed for 12 slot/10 pole motor, ferrite magnets, constant output power of 500 W at constant RMS value of line-to-line voltage 200 V.

Conclusion

The results presented in the paper clearly show potential of the presented interior PM machine with buried ferrite magnets in the rotor construction for applications where high torque density at low speed and wide speed-range with constant output power is required. Although the machine with ferrite magnets and aluminium wire has bigger machine volume, the axial length of the machine can be decreased significantly if higher current limit of the existent power electronics can be taken into account.

REFERENCES
[1] J. Cros and P. Viarouge, Synthesis of high performance PM motors with concentrated windings, *IEEE Transactions on Energy Conversion*, (2001), 248-253.
[2] B. Štumberger et al., High-performance permanent magnet brushless motor with balanced concentrated windings and similar slot and pole numbers, *Journal of Magnetism and Magnetic Materials, 304, no.2,* (2006), e829-e831.
[3] B. Štumberger et al., Determination of the adequate split ratio for high-efficiency permanent magnet synchronous motors with surface mounted magnets and concentrated non-overlapping windings , *Przeglad Electrotechniczny*, 3 (2011), 187-189.
[4] B. Štumberger et al., Modular permanent magnet synchronous motors for wheel hub-drive applications, *Przeglad Electrotechniczny*, 12 (2008), 241-244.
[5] P. Virtič and J. Avsec, Analysis of coreless stator axial flux permanent magnet synchronous generator characteristics by using equivalent circuit, *Przeglad Electrotechniczny*, 3 (2011), 208-211.
[6] P. Virtič, Variations of permanent magnets dimensions in axial flux permanent magnet synchronous machine, *Przeglad Electrotechniczny*, 12b (2011), 194-197.
[7] P. Virtič et al., Torque analysis of an axial flux permanent magnet synchronous machine by using analytical magnetic field calculation, *IEEE Transactions on Magnetics*, 45 (2009), 1036-1039
[8] N. Bianchi and E. Fornasiero, Impact of MMF space harmonics on rotor losses in fractional-slot permanent magnet machines, *IEEE Transactions on Energy Conversion*, (2009), 323-328.
[9] K. Chwastek, Estimation method for the Jiles-Atherton model parameters-a review, *Przeglad Electrotechniczny,* (2008), 145-148.
[10] M. Kuczmann, Measurement and simulation of vector hysteresis, *Przeglad Electrotechniczny,* (2011), 103-106.
[11] M. Kuczmann, Vector Preisach hysteresis modelling: Measurement, identification and application, *Physica B-Condesed Matter,* 406 (2011), 1403-1409.
[12] M. Kuczmann, Measurement and Simulation of Vector Hysteresis Characteristics, *IEEE Transactions on Magnetics,* 4 (2009), 5188-5191.
[13] B. Štumberger and M. Hadžiselimović, Design of permanent magnet synchronous machine for micro-hybrid electric vehicle operation, *Przeglad Electrotechniczny*, 12b (2011), 157-160.
[14] B. Štumberger et al., Design and finite-element analysis of interior permanent magnet synchronous motor with flux barriers, *IEEE Transactions on Magnetics*, 44 (2008), 4389-4392.
[15] B. Štumberger at al., Analysis of iron loss in interior permanent magnet synchronous motor over a wide range of constant output power operation, *IEEE Transactions on Magnetics*, 36 (2000), 1846-1849.
[16] B. Štumberger et al., Accuracy of iron loss calculation in electrical machines by using different iron loss models, *Journal of Magnetism and Magnetic Materials*, 254/255, (2003), 269-271.

Authors: Bojan Štumberger, Miralem Hadžiselimović, Gorazd Hren University of Maribor, Faculty of Energy Technology, Hočevarjev trg 1, 8270 Krško, Slovenia,
E-mail: bojan.stumberger@uni-mb.si.